Remote Sensing in Earth Systems Sciences (2025) 8:1244–1264
https://doi.org/10.1007/s41976-025-00247-y

RESEARCH

Land Use/Land Cover (LULC) Change and Irrigated Area Monitoring in Eritrea: Insights into Horticultural Production and Sustainability

Bereket T. Haile[1] · Abel Ramoelo[1,2] · Andrew J. Dougill[3] · Mcebisi Qabaqaba[1]

Received: 14 July 2025 / Revised: 11 August 2025 / Accepted: 25 August 2025 / Published online: 30 September 2025

Abstract

In arid and semi-arid regions, where water is scarce and climatic variability is high, monitoring changes in irrigated land is essential for ensuring food security and building resilience. However, few studies have assessed irrigation dynamics in the Horn of Africa using remote sensing, and empirical data from Eritrea remain limited. This study investigates the spatio-temporal dynamics of irrigated agriculture in two contrasting regions of Eritrea, Dighe and Gala Nefhi, using multi-temporal Sentinel-2 imagery and Supporting climatic and agricultural datasets from 2015 to 2024. It aims to map the spatial distribution of irrigated fields, assess their changes over time, and examine relationships with rainfall variability, horticultural crop production, and market fluctuations by comparing trends throughout the study period. A supervised Random Forest classification approach was implemented in Google Earth Engine, incorporating spectral indices and post-classification comparison to quantify the Land Use/Land Cover (LULC) transitions. The classification was based on dry-season imagery to distinguish irrigated from rainfed areas, with seven LULC classes identified. Overall classification accuracy ranged from 0.82–0.86 in Dighe and 0.87–0.89 in Gala Nefhi, with Kappa coefficients of 0.70–0.81 and 0.85–0.86, respectively. Results show a 115.5% increase in irrigated area in Dighe and 65.6% in Gala Nefhi. While Gala Nefhi showed synchronized growth in irrigation and horticultural crop production, Dighe exhibited inconsistent yields despite expanded irrigation. The study shows that expanding irrigation alone cannot increase production without reliable water sources, favorable climate conditions, and institutional support.

Keywords Remote sensing · LULC change · Irrigated area · Horticulture · Rainfall variability · Eritrea

1 Introduction

Land Use/Land Cover (LULC) change analysis plays a crucial role in environmental sustainability studies by providing critical insights into landscape transformations driven by anthropogenic and natural factors [45, 63]. Advances in remote sensing technologies have improved LULC monitoring by delivering accurate, repeatable, and cost-effective data over large areas [1, 24, 37]. High-resolution imagery, machine learning algorithms, and cloud-based platforms like Google Earth Engine (GEE) now enable scalable, multi-temporal analyses and the integration of spectral indices to enhance classification accuracy [5, 29, 59, 69]. These developments underscore the increasing potential of satellite remote sensing to systematically capture land cover changes, emphasizing the need for its wider application in monitoring irrigated agriculture in data-scarce regions, where empirical evidence concerning spatial dynamics and the sustainability of land use remains limited.

Monitoring irrigated agriculture, which is vital for horticultural production in Sub-Saharan Africa, is crucial for ensuring food security, effective water management, and ecosystem sustainability [65, 68]. However, mapping irrigated fields using remotely sensed data at the local level remains limited [70], and global datasets are too coarse for local planning [30]. As a result, the extent and rate of change in irrigated areas in data-scarce and fragmented farming systems are poorly understood, which constrains effective resource allocation.

✉ Bereket T. Haile
u22904507@tuks.co.za

[1] Department of Geography, Geoinformatics and Meteorology, University of Pretoria, Pretoria, South Africa

[2] Earth Observation Programme, South African National Space Agency (SANSA), Pretoria 0001, South Africa

[3] Department of Environment and Geography, University of York, University of York, York, UK

Satellite remote sensing offers an efficient way to monitor irrigated lands using sensors such as Landsat, SPOT, MODIS, and Sentinel-1/2 [7, 20, 67]. However, mapping accuracy can be impacted by sensor resolution, spectral confusion with rainfed crops, and different irrigation practices [55]. Researchers have highlighted the value of using ancillary datasets such as precipitation, evapotranspiration, and crop calendars to support the interpretation of classification results, thereby enhancing the reliability of mapping outputs [35]. These inputs help capture when and where farmers irrigate, reducing misclassification and improving the use of remote sensing for irrigation monitoring.

In most African countries, the area under irrigation is traditionally measured through field surveys and reports from local administrative offices. While useful at small scales, these methods are labor-intensive, costly, and often impractical for national or regional-scale monitoring. The application of high-resolution remote sensing technologies for irrigation monitoring in sub-Saharan Africa remains limited due to inadequate digital infrastructure, technical capacity, and financial resources [9, 45]. Hence, most LULC studies in Africa have focused broadly on agricultural land [27, 49, 50, 62], with relatively few efforts to isolate irrigated areas or understand their patterns of change. However, some emerging studies, e.g., Mohammed et al. [44], Muluneh et al. [48] have demonstrated the value of using remote sensing and GIS to quantify the extent, type, and temporal dynamics of irrigation, and to link these changes with climatic, socio-economic, and policy drivers.

In the context of Eritrea, previous LULC studies have focused on broad land cover categories such as forest cover, land degradation, water balance, or general transition in agricultural land, without treating irrigated land as a distinct class or primary focus of analysis [23, 40, 51]. Consequently, there is limited empirical evidence on the transition and drivers of irrigated land expansion. This study addresses this gap by applying multi-temporal Sentinel-2 imagery and Random Forest classification to map irrigated land changes in two sub zobas (sub provinces), Dighe and Gala Nefhi, between 2015 and 2024. Beyond spatial analysis, it integrates horticultural yield data, rainfall anomalies, price trends, and policy developments across this time to examine how irrigation expansion aligns with production dynamics and broader land use transitions. In doing so, the study contributes to the limited body of research on irrigation-focused LULC change in the Sub-Saharan Africa region and provides practical insights for sustainable land and water resource management in Eritrea.

In this study, irrigated land refers to land under full or supplemental irrigation used for horticultural crop production, as identified through LULC classification of multi-temporal satellite imagery. Given the country's semi-arid climate and unreliable rainfall patterns, nearly all horticultural crop production in Eritrea is conducted under irrigation. To guide the investigation, the study adopts a conceptual framework that positions the area under irrigated horticulture at the intersection of multiple influencing factors. These include environmental drivers, economic and social incentives, policy interventions, and infrastructural conditions (Fig. 1). By integrating these dimensions, the study not only quantifies changes in irrigated land but also link them within a broader socio-environmental and institutional context.

The primary aim of this study is to quantify the changes in irrigated land over time and assess its link with the productivity of horticultural crops, land management, and sustainability in Eritrea. Specifically, this research will: (a) examine the spatial distribution of irrigated fields and change over time using multi-temporal remote sensing data and machine learning-based classification techniques (b) assess how changes in irrigated area relate to rainfall variability, horticultural crop production, socio-economic conditions, and policy shifts by comparing patterns and trends across the study period.

By addressing these objectives, this study will enhance the literature on the application of remote sensing for monitoring irrigated agriculture. It will provide empirical insights into sustainable land and water management and support evidence-based policy interventions in agricultural planning.

2 Methodology

2.1 Study Area

Eritrea, located in the Horn of Africa, has a diverse landscape with varying climatic conditions, ranging from arid lowlands to moist highlands [23, 43]. Agriculture is a key sector, with irrigation playing a crucial role in ensuring food security, particularly in the production of horticultural crops [17, 19]. The country is divided into six administrative regions, known as zobas.

This study focuses on Dighe and Gala Nefhi, two sub zobas with contrasting agroecological, hydrological, and socio-economic characteristics (Fig. 2). Dighe, located in the western lowlands, lies within the Barka–Anseba catchment, one of Eritrea's major drainage basins [41, 47]. The area is arid, with erratic annual rainfall ranging between 150–300 mm and average temperatures around 30 °C [14, 25]. Surface water sources are limited to the seasonal River Barka and its tributaries, which flow only during the rainy season [47]. Due to the flat terrain and high infiltration in coarse sandy soils, dam construction is not feasible. As a result, groundwater is the dominant irrigation source, accessed through hand-dug wells and boreholes tapping into unconsolidated alluvial aquifers. These aquifers have varying development potential and salinity levels that often

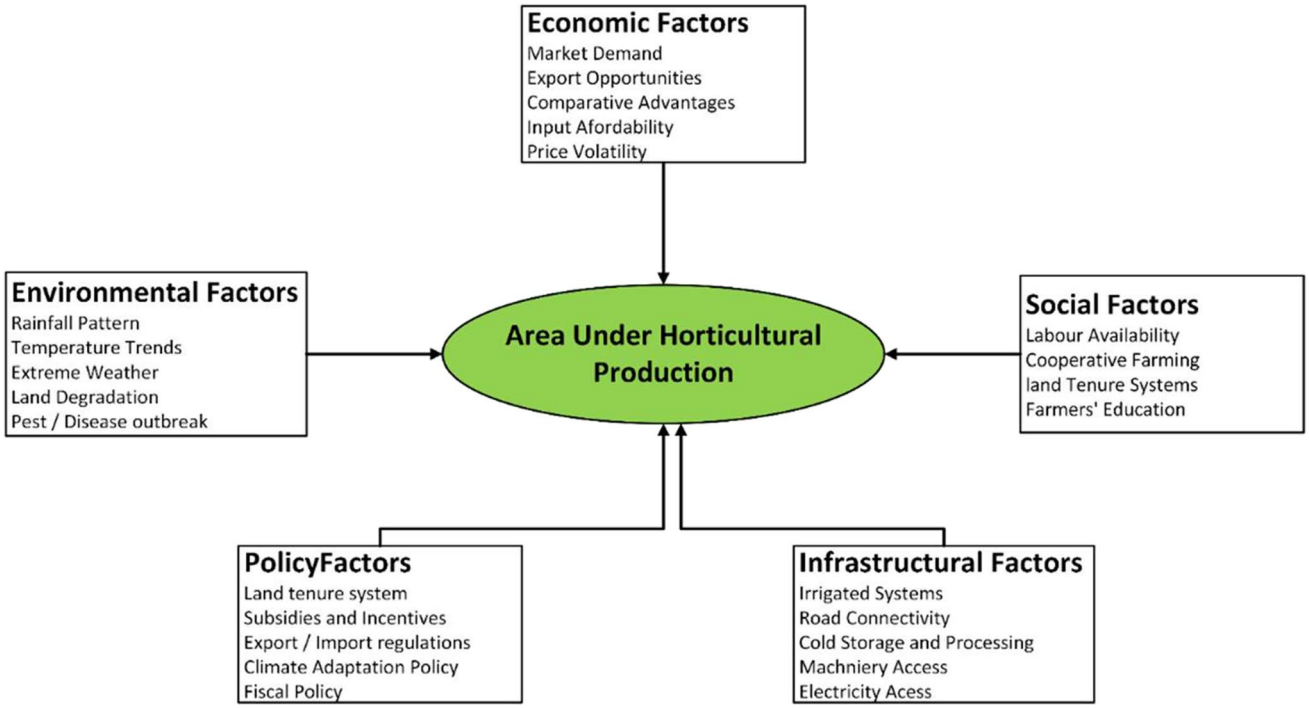

Fig. 1 Conceptual framework illustrating the key environmental, economic, social, policy, and infrastructural factors influencing the area under horticultural crop production, developed by the authors

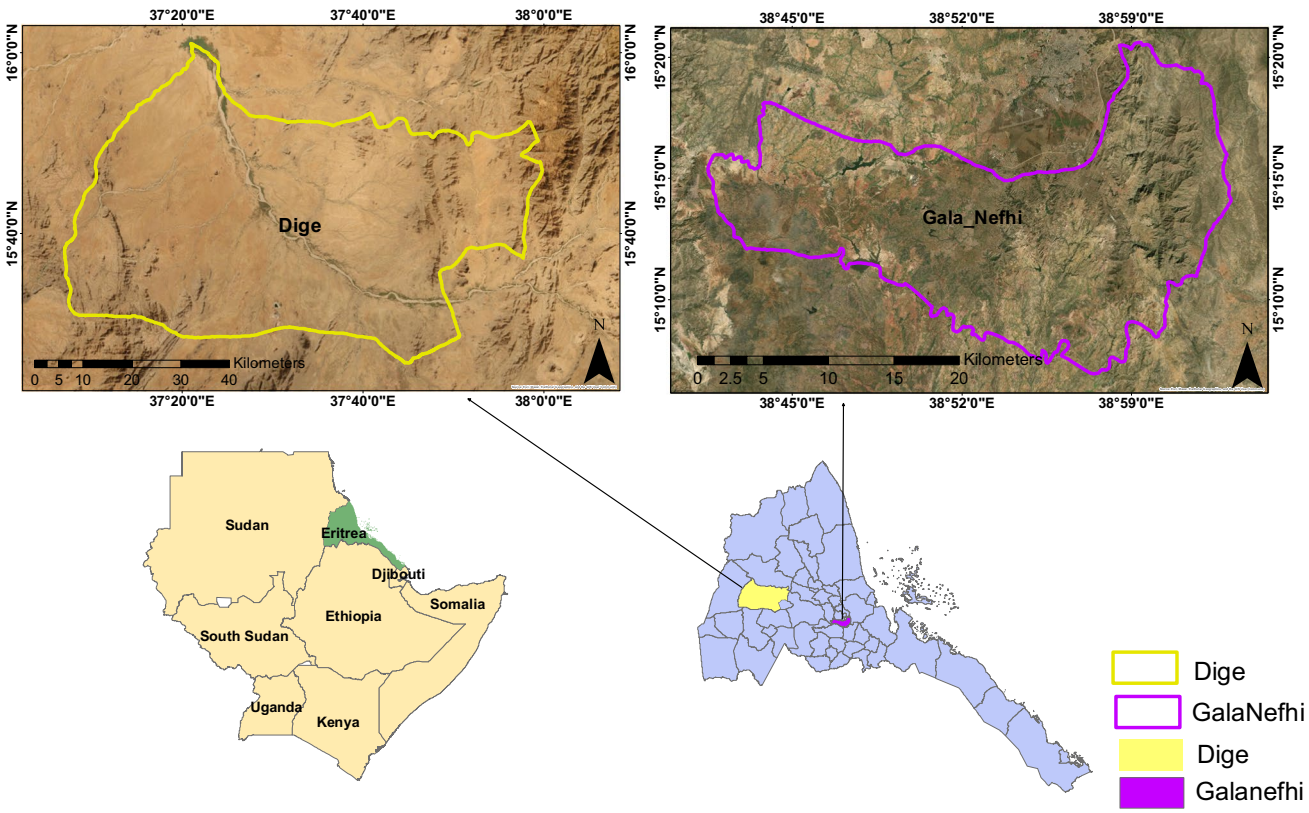

Fig. 2 Eritrea, showing the location of the study area, Dighe and Gala Nefhi

increase with depth and distance from riverbeds [17]. Horticultural farms are concentrated along riverbanks, cultivating seasonal crops such as onion and tomato, as well as perennials like banana and citrus [25, 42].

In contrast, Gala Nefhi is situated in the central highlands, which receive 450–800 mm of annual rainfall and experience a cooler average temperature of 22 °C [52]. Irrigation is primarily based on Surface water stored in over 40 small to medium-sized micro-dams, constructed by the government and communities in recent decades [42]. When reservoir levels are adequate, farmers can cultivate up to three cropping seasons per year. Due to the fissured volcanic and crystalline basement aquifers, it has limited groundwater yield and recharge potential compared to the alluvial systems of the western lowlands [41]. Most farmers use furrow irrigation with diesel pumps to grow mainly potatoes and leafy vegetables [25].

Dighe and Gala Nefhi are the highest horticultural-producing sub zobas in their respective regions [42], and their contrasting environmental and socio-economic contexts make them ideal for a comparative analysis of irrigated land transformation in Eritrea.

2.2 Data Acquisition

2.2.1 Sentinel-2 Data Acquisition and Processing

This study utilized Sentinel-2 Level-2A Bottom-of-Atmosphere (BOA) reflectance imagery for the years 2015, 2018, 2021, and 2024, obtained from Google Earth Engine (GEE), to analyze LULC changes. Since Level-2A products include atmospheric, radiometric, and geometric corrections, additional preprocessing in this study was limited to cloud masking and the selection of clear-sky images to improve classification accuracy [29, 44]. The study period (2015–2024) was selected based on the availability of disaggregated horticulture production data at Sub zoba level by crop type, which is only available from 2015 onward. A three-year interval was adopted to balance the need for detecting medium-term land use changes, giving enough time between images to detect real land use changes rather than seasonal and short-term variations.

To ensure clear differentiation between irrigated and rainfed fields, all satellite images were acquired during January or February of each respective year, which corresponds to the dry season. This timing maximizes spectral contrast and separability, as rainfed fields are typically fallow, while irrigated plots retain active vegetation due to continued water application. It also reduces confusion with natural vegetation and cloud cover, which is common during the wet season. This approach is particularly suitable for arid/semi-arid regions like Eritrea, where there are clear distinctions between irrigated and non-irrigated land during dry months.

2.2.2 Training Data

Ground truth data for training the Random Forest classifier were obtained from two complementary sources. First, high-resolution imagery from Google Earth and historical satellite archives was visually interpreted to digitize all representative LULC classes across the study periods (Table 1). Second, additional training points were collected during a field Survey in June 2024, where GPS-referenced observations were recorded to confirm irrigation status, crop type, and field boundaries. These combined datasets enhanced the accuracy and representativeness of the classification. The dataset was randomly divided into two subsets: training (70%) and validation (30%). To minimise the influence of spatial autocorrelation, training points were sampled in R using the spsample() function with a minimum spacing of 350 m between points. This distance threshold helped maintain spatial independence between training and validation samples. This separation ensured that the data points used to assess the model's accuracy were located in different areas from those used for training, maintaining statistical independence and minimizing spatial overlap between the

Table 1 LULC classes used in the study area

	LULC Class	Description
1	Bare land	Exposed soil, rocky surfaces, degraded land with no or very little vegetation
2	Built-up	Residential, industrial, socio-economic infrastructure, rural houses and mixed urban settlements, roads, and other infrastructures
3	Grazing land	Where the dominant vegetation is grasses, used for grazing animals, with minimal tree (shrubs) cover, typically characterized by open, herbaceous plant communities with less tree and shrub cover
4	Irrigated land	Agricultural land that relies on irrigation water supply systems, ensuring consistent moisture availability for crop growth regardless of natural precipitation
5	Rainfed agriculture	Agricultural lands dependent on rainfall for crop growth, typically characterized by seasonal water availability and varying productivity due to rainfall variability
6	Trees/forest	Areas dominated by dense woody vegetation, including natural forests, woodlands, and planted trees
7	Water bodies	Lakes, reservoirs, and rivers

two sets. Table 2 summarizes the number of training and validation samples used for each LULC class and year in both study areas.

2.2.3 Rainfall Data Acquisition and Variability Assessment

In addition to remote sensing data, rainfall was incorporated as a key climatic variable to assess its influence on irrigated land. Long-term annual rainfall records (1996–2024) were obtained from the Ministry of Agriculture, based on data from three rain gauge stations in Dighe and four in Gala Nefhi. Station-level values were averaged to derive annual rainfall for each sub zoba. Rain gauge station data were used due to their higher reliability and the limited validation of satellite-derived products like CHIRPS, which face accuracy challenges in Eritrea due to sparse and inconsistent in-situ measurements. To evaluate both climatic variability and deviations from historical norms, two complementary metrics were used: the Coefficient of Variation (CV) and the Standardized Rainfall Anomaly (SRA). The use of SRA and CV provides a more comprehensive view of rainfall dynamics, where CV reflects overall variability and SRA highlights annual anomalies. This facilitates better contextualization of rainfall conditions.

CV captures the relative inter-annual variability during the study period (2015–2024) and was calculated using Eq. 1:

$$CV = \left(\frac{\sigma}{\mu}\right) \times 100 \quad (1)$$

where;

σ is the standard deviation.

μ is the mean annual rainfall.

SRA, which requires a long-term baseline, was computed using data from 1996 to 2024 to assess whether a given year was wetter or drier than average. It was calculated using Eq. (2):

$$SRA_t = \frac{P_t - \mu}{\sigma} \quad (2)$$

where;

P_t is the rainfall in year t.

σ is the standard deviation (1996–2024).

μ is the long-term mean annual rainfall (1996–2024).

2.2.4 Horticultural Production and Market Price Data

Total horticultural production data for Dighe and Gala Nefhi Sub zobas, covering the period from 2015 to 2024, were obtained from the Ministry of Agriculture's database to examine how irrigation expansion aligns with crop yield trends.

To examine how market dynamics relate to irrigation expansion and production trends, a Horticultural Price Index was used as an analytical tool. A price index is a standard

Table 2 Number of training and validation points used for supervised classification of each LULC class across the study period in Dighe and Gala Nefhi

Sub Zoba	LULC Class	2015		2018		2021		2024	
		Training	Validation	Training	Validation	Training	Validation	Training	Validation
Dighe	Bare land	811	339	810	357	788	358	800	346
	Built-up	51	25	89	50	146	65	191	72
	Grazing land	2037	813	2030	812	1970	872	2028	804
	Irrigated land	208	99	250	105	336	157	406	173
	Rainfed agriculture	327	120	389	158	388	187	442	159
	Trees/forest	173	79	237	79	303	130	293	147
	Water bodies	18	11	20	9	44	10	58	19
Gala Nefhi	Bare land	573	214	540	241	544	237	560	221
	Built-up	1366	546	1460	622	1474	607	1371	628
	Grazing land	717	321	722	308	740	290	707	323
	Irrigated land	658	293	721	321	802	296	743	333
	Rainfed agriculture	1237	561	1208	592	1292	508	1238	562
	Trees/forest	1112	466	1077	501	1095	483	1126	453
	Water bodies	688	283	641	312	675	271	704	286

economic tool used to track changes in the average prices of a defined basket of goods over time [18]. In agricultural research, it is commonly used to assess profitability trends, supply responses, and market conditions influencing land use and production decisions [8, 36]. By smoothing out annual price fluctuations, the index enables a more meaningful comparison between economic conditions, irrigated area, and total horticultural output, offering insight into whether observed production changes are economically driven.

A Horticultural Price Index was developed using the five most widely produced crops in the area; tomato, onion, potato, cabbage, and banana, selected for their consistent dominance in local horticultural output during the study period. Market price data, specifically mean annual prices in Nakfa (ERN), the national currency of Eritrea, per kilogram, were sourced from the Ministry of Agriculture Strategic Information Division based on records from the Asmara wholesale market, the main outlet for produce from Dighe and Gala Nefhi. The index was calculated as a simple unweighted average, with 2015 as the base year.

The average price level of the selected horticultural crops in year t (Price Index t) is calculated using Eq. (3).

$$Price\ Index_t = \left(\frac{\overline{P}_t}{\overline{P}_{2015}}\right) \times 100 \tag{3}$$

where:

P_t average price of the five selected crops in year t

P_{2015} average price of the five crops in the base year (2015)

2.3 Land Use/Land Cover Classification

A supervised classification approach was employed using the Random Forest (RF) algorithm, a recognized classification technique known for its high accuracy and robustness in handling large datasets [16, 29, 35]. The classification process was done in Google Earth Engine (GEE), followed by post-classification refinements to minimize errors and misclassifications.

To improve classification accuracy and enhance class separability, a set of spectral indices was included as additional input features. These indices were deliberately selected based on their relevance to the spectral characteristics of the target land cover classes (see Table 3). Testing the model with and without spectral indices showed that their inclusion improved overall classification accuracy, confirming their role in enhancing feature separability. Gu & Zeng [24], Mohammed et al. [44], Xiang et al. [72] are examples of studies that effectively used spectral indices in the identification of irrigated fields.

2.4 Accuracy Assessment

The classification accuracy was evaluated using a confusion (error) matrix, which compared the classified images with reference data. The accuracy assessment considered key performance metrics, including Overall Accuracy, percentage of correctly classified pixels (Eq. (4)), and Kappa Coefficient, a measure of agreement beyond chance (Eq. (5)) [10]. The Kappa Coefficient has been, and continues to be, widely used in LULC classification studies as a standard metric to evaluate the agreement between classified maps and reference data while accounting for chance agreement [12, 33, 39]. Despite its broad application, some scholars have critiqued its usefulness, noting that it is often highly correlated with overall accuracy and may offer limited additional insight [21]. Others also critique Kappa for combining quantity and spatial allocation errors into a single metric, which can obscure the true nature of classification inaccuracies [57]. To address these limitations and better understand the performance of individual classes, user's and producer's accuracies were computed for each year (Eqs. (6) and (7)), providing a more detailed evaluation of classification reliability at the class level.

Table 3 Indices used in the study to improve the classification

	Index	Formula	Source
1	Normalized Difference Vegetation Index (NDVI)	$NDVI = \frac{(NIR-Red)}{(NIR+Red)}$	Rouse et al. [61]
2	Enhanced Vegetation Index (EVI)	$EVI = 2.5\frac{(NIR-Red)}{(NIR)+(6Red-7.5\,Blue)+1}$	Huete et al. [26]
3	Optimized Soil-Adjusted Vegetation Index (OSAVI)	$OSAVI = \frac{(NIR-Green)}{(NIR+Red)+0.16}$	Rondeaux et al. [60]
4	Leaf Area Index (LAI)	$LAI = -ln\left(\frac{NDVI\max-NDVI}{NDVI\max-NDVI\,min}\right) \div k$	[6]
5	Normalized Difference Built-up Index (NDBI)	$NDBI = \frac{SWIR-NIR}{SWIR+NIR}$	Zha et al. [76]
6	Normalized Difference Water Index (NDWI)	$NDWI = \frac{Green-NIR}{Green+NIR}$	McFEETERS, [38]
7	Modified Normalized Difference Water Index (MNDWI)	$MNDWI = \frac{Green-SWIR}{Green+SWIR}$	Xu, [73]

$$Overall\,Accuracy = \frac{Sum\ of\ major\ diagonal}{Sum\ of\ total\ correct\ pixels}\ x\,100 \quad (4)$$

$$Kappa\,Coeffficient = \frac{Observed\ accuracy\ (Po) - Chance\ agreement\ (Pe)}{1 - Chance\ Agreement\ (Pe)}\ x\,100 \quad (5)$$

$$Producer's\,Accuracy = \frac{Samples\ correctly\ identified\ in\ the\ column}{Colunm\ Total}\ x\,100 \quad (6)$$

$$User's\,Accuracy = \frac{Samples\ correctly\ identified\ in\ the\ row}{Row\ Total}\ x\,100 \quad (7)$$

2.5 Land Use/Land Cover Change Detection Analysis

The analysis of LULC change was conducted using a combination of GEE for classification and R Statistical software version 4.1.3 [58] for quantitative change assessment. After obtaining the final classified maps from GEE, a comparative analysis was performed to assess the percentage change in land cover area across different periods. The percentage change in area for each LULC class was calculated for the periods 2015–2018, 2015–2021, and 2015–2024, enabling the identification of trends and the major periods of change across this period. To give a better understanding of the temporal change patterns of irrigated area, the Sen slope estimator was applied, calculating the median rate of change across all pairwise intervals.

To further analyze the spatial dynamics of LULC transitions, a Post-Classification Comparison (PCC) technique was applied to generate a LULC change transition matrix. This matrix, computed for 2015–2024, provides a detailed "from-to" change assessment, capturing the extent of conversions between land cover classes, such as the expansion or contraction of irrigated areas, agricultural intensification, and loss of natural vegetation. PCC provides a pixel-level comparison across classified maps, thereby eliminating the need for radiometric normalization between dates. It also facilitates the quantification of specific land cover conversions, which is crucial for understanding land dynamics over time [28]. The cross-tabulation matrix and associated loss and gain statistics were calculated in R providing a more detailed understanding of landscape transformations. Additionally, an error matrix was computed to assess classification accuracy and validate the reliability of the detected changes.

To quantify the rate and direction of land cover transitions across various LULC classes during the study period, a rate of change was calculated using Eq. (8).

$$r = \left(\frac{1}{t_2 - t_1}\right) \times ln\left(\frac{A_2}{A_1}\right) \quad (8)$$

r = Rate of Change, *A1* and *A2* are land cover at time t_1 and t_2 per year.

2.6 Data Analysis

The study employed a comparative trend analysis to examine how changes in horticultural production, rainfall variability, and market prices relate to the expansion of irrigated land over time. By analyzing the direction and rate of change across these variables, the study offers a better understanding of the factors influencing irrigated agriculture in the study areas. Although rainfall, production, and price index data were available for nine years, the irrigated area was derived from LULC classification for only four years (2015, 2018, 2021, and 2024). Due to the limited number of observations for the irrigated area, no formal statistical tests were applied to assess correlation or causality between the irrigated area and the other variables (Fig. 3). However, to assess potential relationships between rainfall variability and observed production trends, an exploratory Pearson correlation analysis was conducted for each sub-zoba.

3 Results

3.1 Accuracy Assessment

The overall and class-level accuracy was generally high, with notable consistency observed in the classification of water bodies and irrigated areas. In contrast, Built-up and

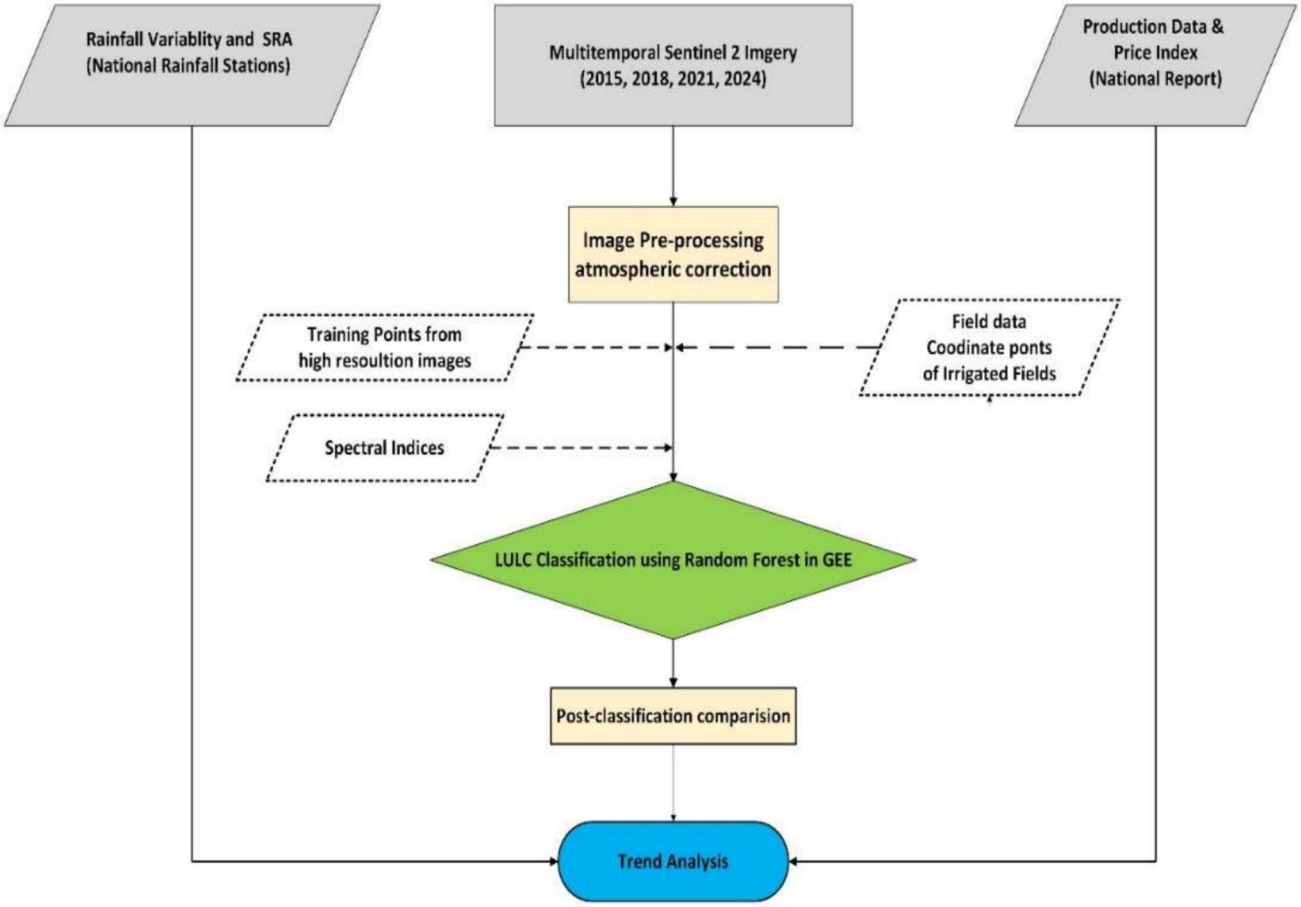

Fig. 3 Workflow for LULC classification and trend analysis integrating Sentinel-2 imagery, field data, and agricultural statistics using Random Forest in GEE

Grazing land showed relatively low and inconsistent accuracy levels (Table 4).

3.2 LULC Change Dynamics

During the study period, grazing land was the dominant LULC class in both sub zobas. Rainfed agriculture also remained a major land cover type across the two sub zobas, followed by varying levels of bare land in Dighe and built-up areas in Gala Nefhi (see Tables 5 and 6). With minor fluctuations, tree and forest cover remained relatively stable across both Sub zobas. Irrigated land increased by 115.5% in Dighe and 65.6% in Gala Nefhi, with annual growth rates of 8.53% and 5.60% respectively (Tables 5 and 6), reflecting a shift toward more intensive horticultural production.

The LULC classification maps for Gala Nefhi and Dighe from 2015 to 2024 (Figs. 4 and 5) illustrate distinct spatial patterns and temporal dynamics across the study period. In Gala Nefhi, a noticeable expansion in irrigated land (green) is evident, particularly between 2018 and 2021, accompanied by a gradual reduction in rainfed agriculture and bare land. Dighe, irrigated areas are mainly concentrated along the Barka River (seasonal river). These maps visually support the observed quantitative changes and confirm the differing land transformation trajectories in the two sub zobas.

3.3 Land Use/Land Cover Change Matrix (transition)

The Land Use/Land Cover (LULC) transition matrix between 2015 and 2024 reveals notable spatial dynamics in both Dighe and Gala Nefhi (Tables 7 and 8). Irrigated area in Dighe displays a net gain of 54.4 km^2, showing improved persistence and expansion. Gala Nefhi also gains 13.87 km^2 of irrigated area and a net loss in traditional land uses like rainfed agriculture and grazing (Fig. 6). The Sen slope analysis indicated an annual increase of 5.56 km^2/year in Dighe and 1.55 km^2/year in Gala Nefhi. These rates complement

Table 4 Overall accuracy, Kappa coefficient, user's and producer's accuracy (%) for each LULC class across the study period in Dighe and Gala Nefhi

Sub Zoba	Year	Accuracy	LULC classes						
			Bare land	Built up	Grazing Land	Irrigated Area	Rainfed Agriculture	Trees/Forest	Water
Dighe	2015	Producer's	59.29	12.00	92.37	93.94	75.83	89.87	100.00
		User's	72.56	100.00	82.80	90.29	79.82	100.00	100.00
		Overall	0.82						
		Kappa	0.71						
	2018	Producer's	68.07	30.00	90.89	83.81	82.28	96.20	100.00
		User's	73.19	88.24	85.02	87.13	79.27	96.20	100.00
		Overall	0.83						
		Kappa	0.73						
	2021	Producer's	73.18	43.08	93.58	84.08	76.47	84.62	100.00
		User's	79.39	68.29	85.27	85.16	85.12	93.22	100.00
		Overall	0.84						
		Kappa	0.77						
	2024	Producer's	71.10	70.83	92.79	84.97	91.19	89.80	94.74
		User's	81.19	86.44	86.54	87.50	83.33	97.06	100.00
		Overall	0.86						
		Kappa	0.81						
Gala Nefhi	2015	Producer's	84.11	90.29	74.77	81.91	96.61	85.41	95.41
		User's	89.55	92.15	73.85	83.04	87.70	90.45	97.83
		Overall	0.88						
		Kappa	0.86						
	2018	Producer's	85.89	92.44	72.40	78.50	96.28	85.03	94.55
		User's	91.19	91.13	71.47	80.25	88.92	90.25	98.33
		Overall	0.88						
		Kappa	0.86						
	2021	Producer's	84.39	90.94	68.28	83.11	94.69	87.16	94.46
		User's	90.91	89.61	76.74	81.46	86.51	87.71	98.46
		Overall	0.87						
		Kappa	0.85						
	2024	Producer's	86.88	89.81	78.33	80.48	96.44	88.52	94.06
		User's	94.12	93.38	75.30	85.08	88.13	87.17	98.90
		Overall	0.89						
		Kappa	0.87						

the total percentage increases and confirm the faster expansion in Dighe.

3.3.1 Rainfall Variability

Rainfall variability across the two sub zobas reveals distinct patterns over both the long-term period (1996–2024) and the study period (2015–2024). Over the long term, Gala Nefhi received higher median rainfall than Dighe, with a narrower spread and fewer extreme outliers, suggesting a relatively more stable and wetter climate. Dighe displayed greater interannual variability, reflected in a wider range of rainfall values and a lower median, indicating a drier and less predictable climate. Box plots of the two regions (Fig. 7) confirm these patterns, with Dighe showing a higher frequency of below-average rainfall years.

The Standardized Rainfall Anomaly (SRA) graphs (Fig. 8) illustrate distinct interannual rainfall variability in Dighe and Gala Nefhi from 1996 to 2024. In Dighe, extreme negative anomalies were observed in 2001 and 2002, while

Table 5 LULC change trend and annual rate of change, Dighe

LULC Class	Area in km^2 2015	Area in km^2 2018	Area in km^2 2021	Area in km^2 2024	2015–2018		2018–2021		2021—2024		2015—2024		% Annual change rate (2015–2024)
					Difference	%	Difference	%	Difference	%	Difference	%	
Bare land	1426.81	1410.68	1338.11	1373.80	−16.13	−1.13	−72.57	−5.14	35.69	2.67	−53.0135	−3.72	−0.42
Built-up	4.13	10.28	25.50	32.38	6.15	148.85	15.21	148.00	6.89	27.02	28.2521	683.87	22.88
Grazing land	2102.33	2061.86	2061.79	2056.57	−40.47	−1.92	−0.08	0.00	−5.21	−0.25	−45.7578	−2.18	−0.24
Irrigated land	47.06	85.67	100.90	101.42	38.61	82.04	15.23	17.77	0.52	0.51	54.3561	115.50	8.53
Rainfed agriculture	94.58	101.85	141.56	105.72	7.27	7.69	39.71	38.99	−35.84	−25.32	11.1456	11.78	1.24
Trees/forest	47.53	43.29	47.27	46.29	−4.24	−8.92	3.98	9.20	−0.98	−2.08	−1.2374	−2.60	−0.29
Water bodies	7.30	16.03	14.62	13.56	8.73	119.48	−1.41	−8.82	−1.06	−7.23	6.2549	85.64	6.87

Table 6 LULC change trend and annual rate of change, Gala Nefhi

and Cover Class	Area in km^2 2015	Area in km^2 2018	Area in km^2 2021	Area in km^2 2024	2015–2018		2018–2021		2021–2024		2015–2024		% Annual Change Rate (2015–2024
					Difference	%	Difference	%	Difference	%	Difference	%	
Bare land	23.38	27.85	22.19	18.01	4.47	19.12	−5.66	−20.32	−4.18	−18.84	−5.37	−22.97	−2.9
Built-up	41.85	47.1	46.9	39.09	5.25	12.54	−0.2	−0.42	−7.81	−16.65	−2.76	−6.59	−0.76
Grazing land	143.57	136.84	127.94	142.61	−6.73	−4.69	−8.9	−6.50	14.67	11.47	−0.96	−0.67	−0.08
Irrigated land	21.14	25.66	36.89	35.01	4.52	21.38	11.23	43.76	−1.88	−5.10	13.87	65.61	5.6
Rainfed agriculture	100.39	89.15	90.27	93.89	−11.24	−11.20	1.12	1.26	3.62	4.01	−6.5	−6.47	−0.74
Trees/forest	54.79	59.07	60.77	56.6	4.28	7.81	1.7	2.88	−4.17	−6.86	1.81	3.30	0.36
Water bodies	2.22	1.72	2.5	2.15	−0.5	−22.52	0.78	45.35	−0.35	−14.00	−0.07	−3.15	−0.38

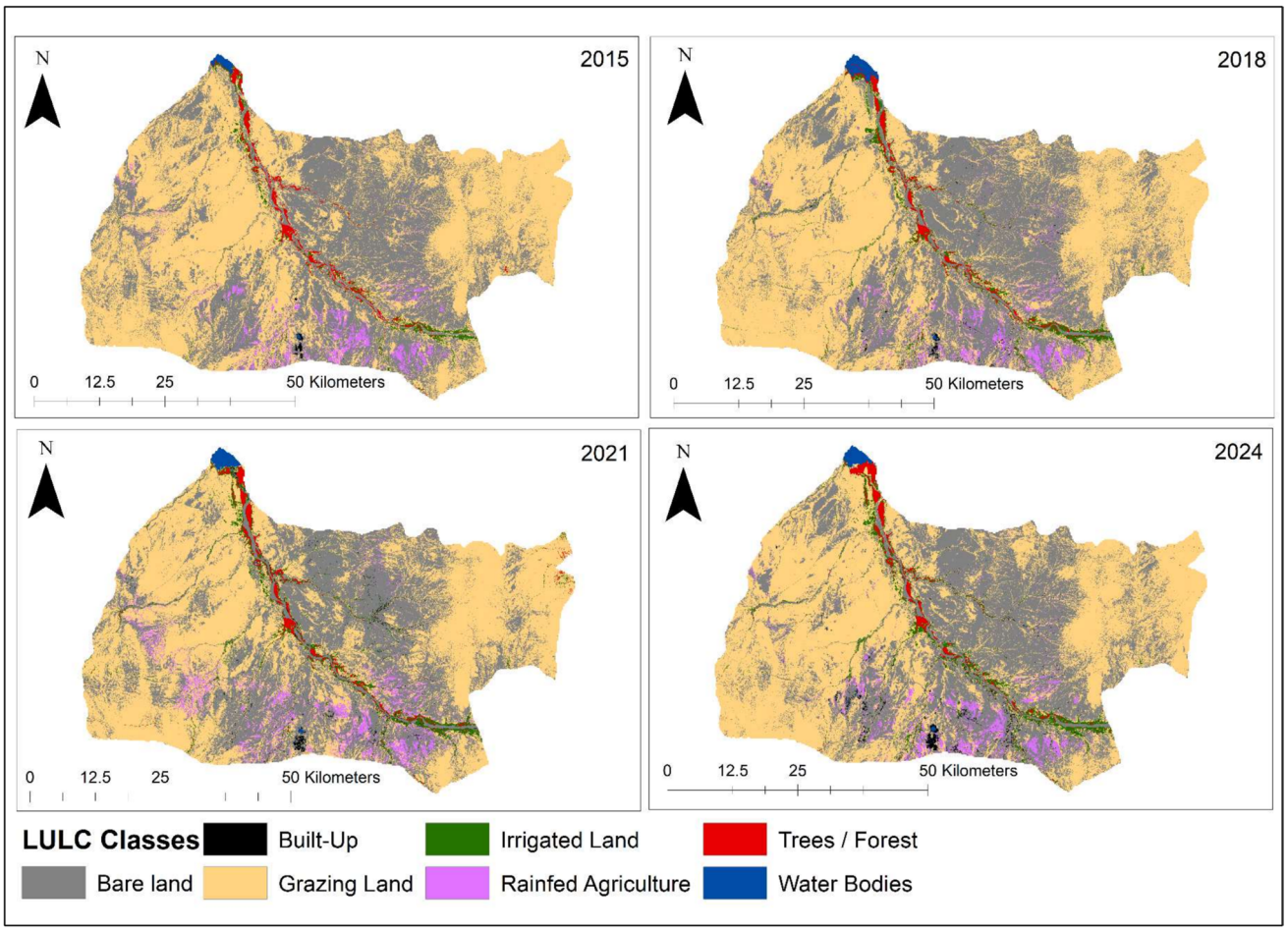

Fig. 4 Land Use/Land Cover classification maps of Dighe for the years 2015, 2018, 2021, and 2024, showing spatial distribution of seven LULC classes, including irrigated land

positive anomalies became more frequent in recent years, with 2019 and 2024 standing out as particularly wet years. Gala Nefhi exhibited Sustained negative anomalies between 2002 and 2013, Suggesting a prolonged dry phase, followed by a recovery trend with strong positive anomalies in 2023 and 2024.

The Coefficient of Variation (CV) analysis provides additional insight into rainfall stability across the two sub zobas. Over the long-term period (1996–2024), Dighe exhibited a higher CV (32.6%) compared to Gala Nefhi (26.2%), suggesting that rainfall in Dighe is more variable and less predictable than in Gala Nefhi. When narrowed to the study period (2015–2024), the CV values slightly decreased in both areas, Dighe at 28.1% and Gala Nefhi at 22.7%, indicating a relatively more stable rainfall regime in recent years, especially in Gala Nefhi. This contrast emphasizes the differing climatic reliability between the arid lowlands of Dighe and the more temperate highlands of Gala Nefhi.

3.3.2 Horticulture Production Trends

During the study period, horticultural production in Dighe showed fluctuations, with total output peaking in 2016 (48,174.5 MT) and 2019 (46,814.5 MT), as shown in Table 9. However, a gradual decline was observed after 2020, with total production decreasing to 41,000 MT by 2024. In contrast, Gala Nefhi exhibited a steady and significant increase in horticultural output, especially in vegetables, rising from 4282.8 MT in 2015 to 8090 MT in 2024.

Figure 9 illustrates the relationship between horticultural production and irrigated area from 2015 to 2024, revealing distinct patterns for the two Sub zobas. In Dighe,

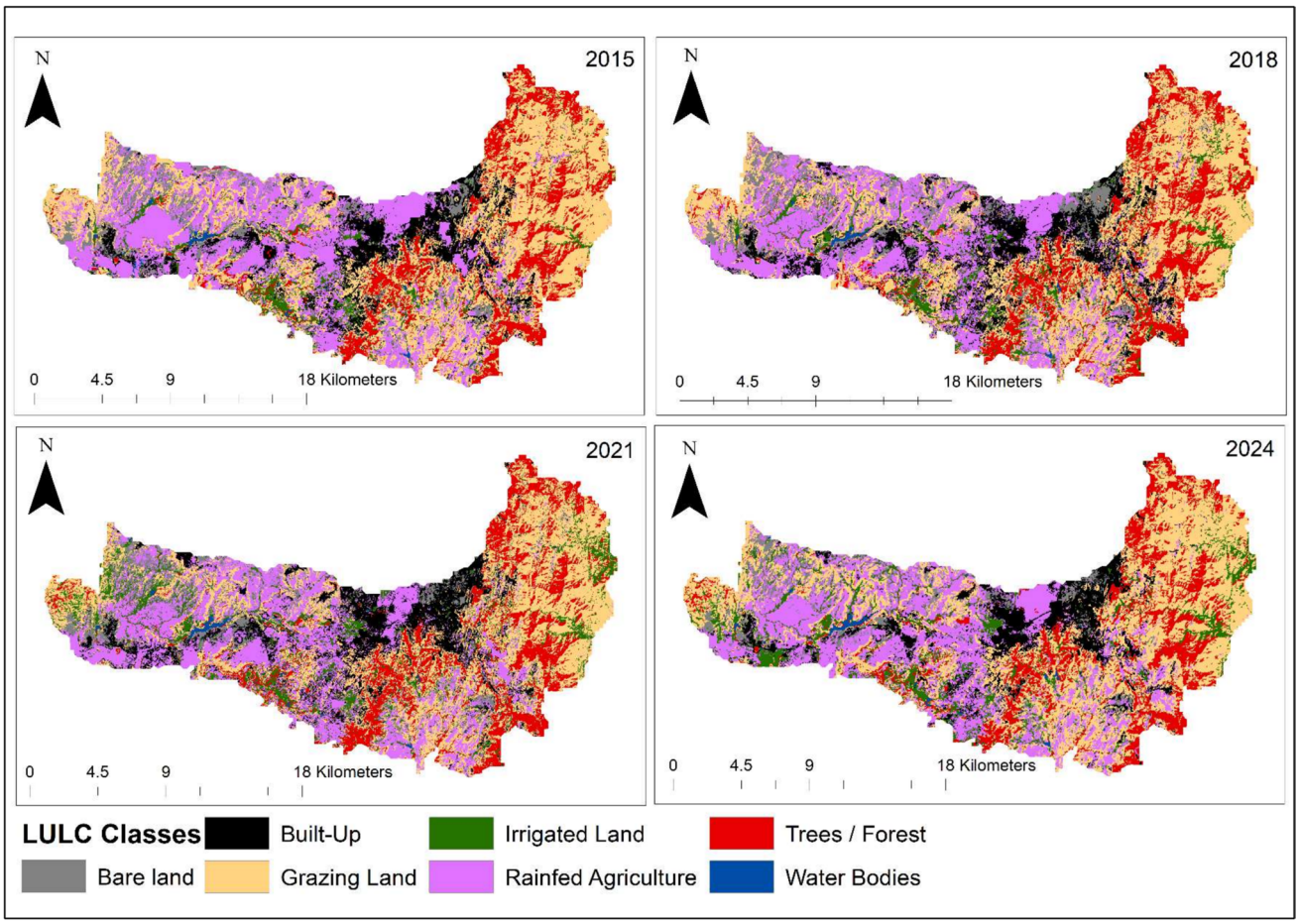

Fig. 5 Land Use/Land Cover classification maps of Gala Nefhi for the years 2015, 2018, 2021, and 2024, showing spatial distribution of seven LULC classes, including irrigated land

Table 7 Dighe LULC change matrix and the net change in terms of gains and losses (2015–2024)

LULC	Bare land	Built-up	Grazing land	Irrigated land	Rainfed agriculture	Trees/forest	Water bodies	Total 2015	Loss
Bare land	1087.89	20.49	269.33	9.76	34.84	2.83	1.67	1426.81	338.92
Built-Up	0.17	2.56	0.87	0.11	0.08	0.01	0.34	4.13	1.58
Grazing Land	261.35	7.88	1754.87	46.74	23.52	5.87	2.10	2102.33	347.46
Irrigated Land	1.68	0.36	5.70	30.61	0.21	7.10	1.40	47.06	16.45
Rainfed Agriculture	21.87	0.71	24.19	0.74	47.06	0.00	0.00	94.58	47.51
Trees/Forest	0.83	0.36	1.50	13.46	0.01	30.14	1.23	47.53	17.39
Water Bodies	0.00	0.03	0.11	0.00	0.00	0.34	6.82	7.30	0.49
Total 2024	1373.80	32.38	2056.57	101.42	105.72	46.29	13.56	3729.74	
Gain	285.91	29.83	301.70	70.80	58.66	16.15	6.74		

while the irrigated area increased significantly, horticultural production fluctuated and even declined slightly after peaking in 2018. Gala Nefhi displays a more positive and synchronized trend between irrigated area and horticultural production.

Pearson correlation analysis indicated a weak, non-significant relationship between annual rainfall and total horticultural production in both sub-zobas: Dighe ($r=0.22$, $p=0.55$) and Gala Nefhi ($r=0.33$, $p=0.35$).

Table 8 Gala Nefhi LULC change matrix and the net change in terms of gains and losses (2015–2024)

LULC	Bare land	Built-up	Grazing land	Irrigated land	Rainfed agriculture	Trees/forest	Water bodies	Total 2015	Loss
Bare land	9.84	3.27	3.21	1.05	5.83	0.11	0.08	23.38	13.54
Built-up	1.77	25.71	5.21	1.16	7.43	0.45	0.11	41.85	16.13
Grazing land	2.04	2.09	114.86	6.38	5.61	12.39	0.19	143.57	28.71
Irrigated land	0.13	0.85	3.88	10.08	4.55	1.40	0.26	21.14	11.06
Rainfed agriculture	4.06	6.90	6.23	12.51	69.69	0.68	0.32	100.39	30.70
Trees/forest	0.10	0.19	8.94	3.32	0.60	41.48	0.15	54.79	13.31
Water bodies	0.06	0.07	0.27	0.51	0.17	0.10	1.03	2.22	1.19
Total 2024	18.01	39.09	142.61	35.01	93.89	56.60	2.15	387.35	
Gain	8.17	13.37	27.74	24.93	24.19	15.12	1.11		

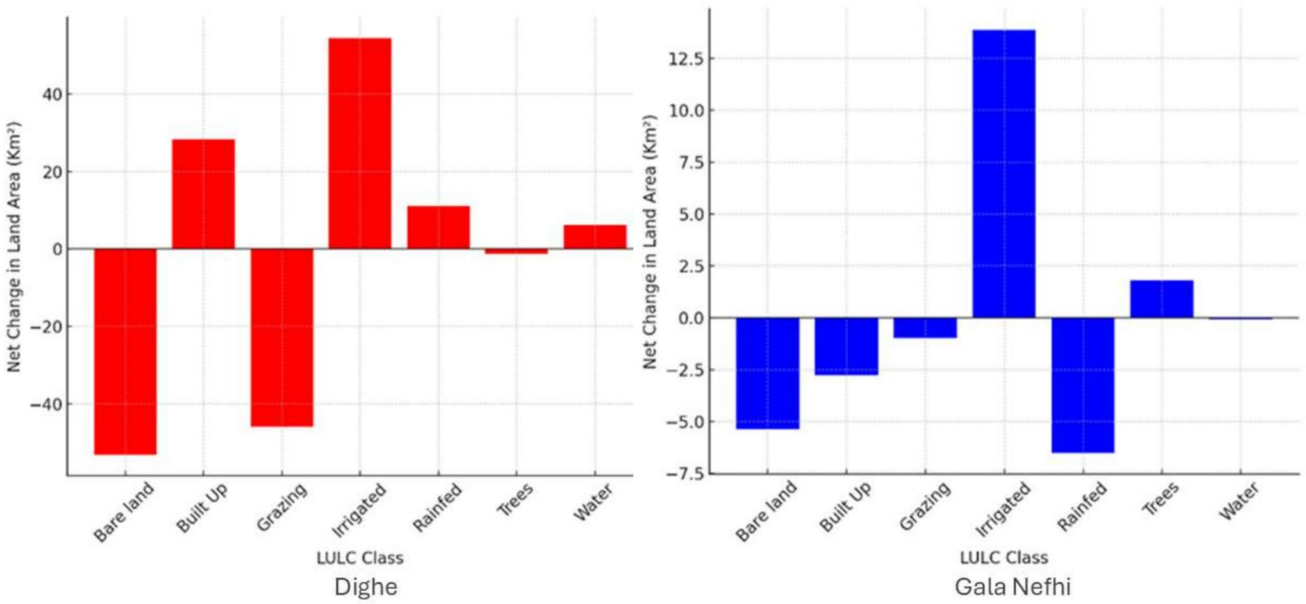

Fig. 6 Net change (gain–loss) for each LULC class 2015–2024

3.3.3 Horticultural Crops Price Index

The horticultural price index, developed using the average annual prices of five major horticultural crops in the country's main market (Fig. 10), consistently declined after 2015, reaching its lowest point between 2019 and 2021 before experiencing a modest recovery.

4 Discussion

This study examined the spatial and temporal expansion of irrigated agriculture in Dighe and Gala Nefhi Sub-zobas of Eritrea from 2015 to 2024 using Sentinel-2 images to analyze its connection with horticultural production, climate variability, and price trends. Satellite images offer a scalable and cost-effective tool for monitoring irrigated land expansion and water use [20], however, their application is often constrained by methodological uncertainties, such as inconsistent validation techniques and variability in reference datasets [22]. Several studies in Africa have effectively used Sentinel-1 and Sentinel-2 imagery to map irrigated areas in smallholder farming systems [32, 53, 74]. This demonstrates their ability to detect small-scale irrigated fields, although very small and fragmented plots might still be overlooked due to resolution limits.

In this study, images were acquired during the dry season, when the spectral contrast between irrigated and rainfed

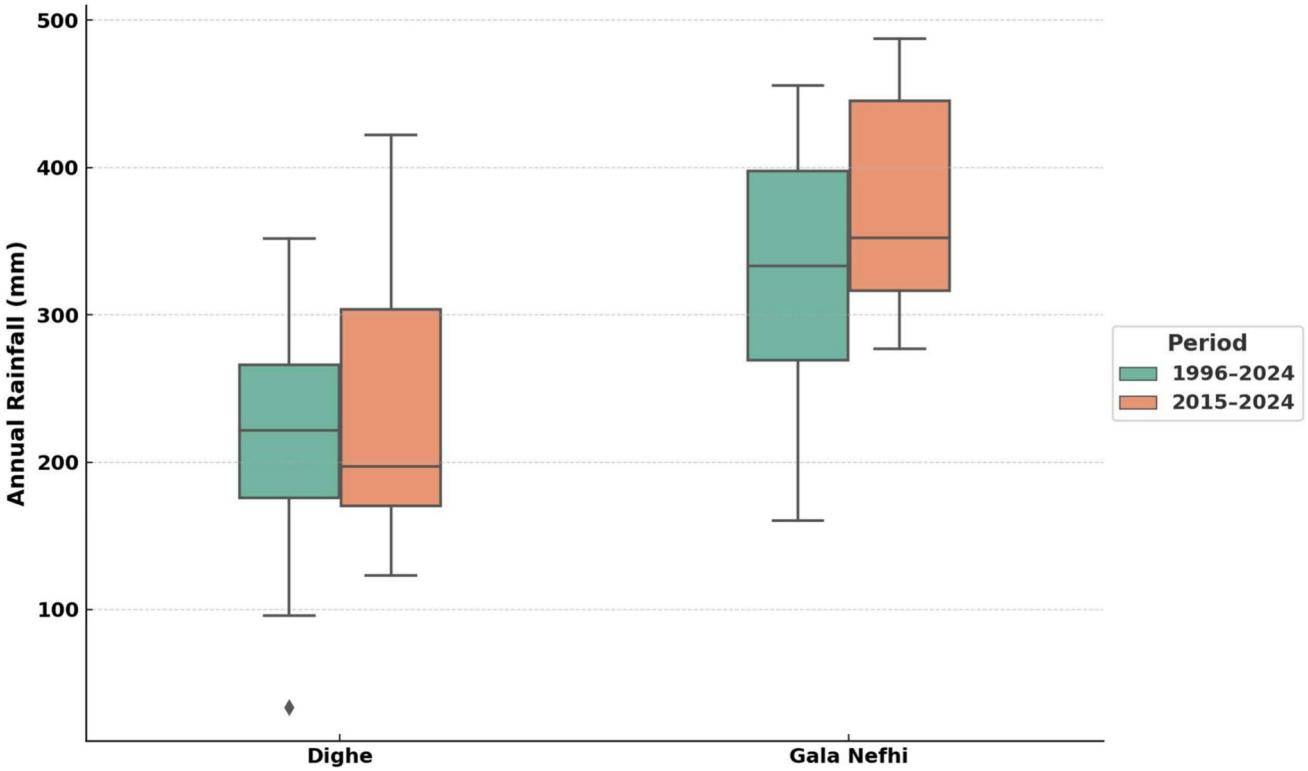

Fig. 7 Boxplot comparison of annual rainfall variability in Dighe and Gala Nefhi sub-zobas for the study period (2015–2024) and the long-term period (1996–2024). Source: Ministry of Agriculture, Eritrea

fields is at its peak. Similarly, a study in Burkina Faso [75] used images of post-harvest months (October–November) to achieve optimum classification results. This shows that remote sensing, combined with agronomic knowledge and additional data, offers reliable information, especially for irrigation mapping, which involves interpreting vegetative signals and understanding farmers' seasonal crop and water management practices [55].

The overall classification exceeded the threshold of 80%, indicating a high level of classification reliability [11, 39]. However, low producers' accuracy in built-up and bare land could be due to spectral confusion between rural structures with soil or thatch roofs and adjacent bare or sparsely vegetated land. This suggests that classes with mixed or transitional spectral signatures are challenging to classify consistently across various spatial and temporal contexts. A similar challenge has been highlighted by [13] and [34] who observed frequent misclassification between classes with similar spectral reflectance. Conversely, irrigated areas demonstrate high classification accuracy, indicating that they are mapped with strong completeness and reliability.

While irrigated area increased in both regions, the link between area expansion and horticultural production was inconsistent, with Dighe displaying production volatility despite irrigation growth. Gala Nefhi showed a more synchronized trend between irrigated area and horticultural output, especially in the later years of the study period. The discrepancy between area expansion and production growth observed in Dighe could be due to differences in the quality or availability of complementary support systems, such as extension services, input access, and farmer training, which significantly enhance productivity outcomes under irrigated conditions. Studies like Dube [15], Koech et al. [31] and Stevens & Ntai [66] have shown that the success of irrigation investments often depends on effective support systems that help farmers adopt and manage irrigation technologies optimally, further reinforcing this hypothesis.

Production response to rainfall varied notably between the two study areas. In Dighe, horticultural output did not consistently align with fluctuations in rainfall or the expansion of irrigated area, whereas in Gala Nefhi, there was a similarity between rainfall trends, irrigation growth, and

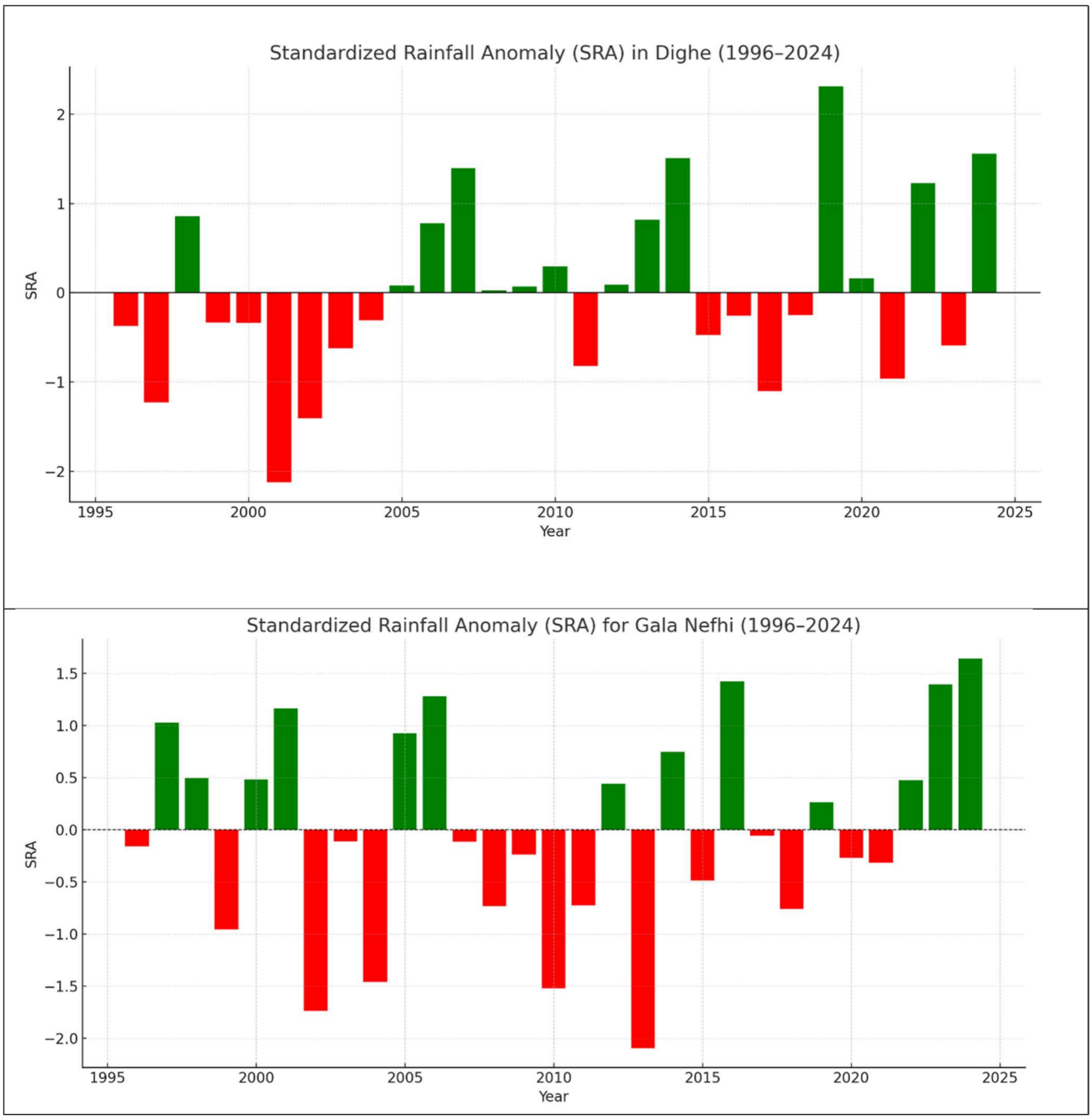

Fig. 8 Standardized Rainfall Anomaly (SRA) trends from 1996 to 2024 for Dighe **a** and Gala Nefhi **b**

increased production, particularly in the earlier years of the study period. The difference in trend is likely linked to differences in irrigation water sources. Dighe relies primarily on groundwater wells, which are less immediately responsive to short-term rainfall variability, while Gala Nefhi depends on micro-dams, making its production more sensitive to interannual rainfall fluctuations. This interpretation is supported by the analysis of Standardized Rainfall Anomaly (SRA) and Coefficient of Variation (CV), which indicates substantial interannual rainfall variability in both locations, with Dighe exhibiting higher long-term climatic unpredictability (CV = 32.6%) compared to Gala Nefhi (CV = 26.2%). Expansion of irrigated area in both sub zobas, shows that the expansion was not directly driven

Table 9 Annual horticultural production (Vegetables and Fruits) in metric tons (mt) for dighe and gala nefhi sub zobas (2015–2024). Source: Ministry of agriculture reports

Year	Dighe		Gala Nefhi		Dighe	Gala Nefhi
	Vegetable (mt)	Fruits (mt)	Vegetable (mt)	Fruits (mt)	Total horticulture (mt)	Total horticulture (mt)
2015	19,980.0	26,830.0	3788.0	494.8	46,810.0	4282.8
2016	20,294.5	27,880.0	3805.0	414.0	48,174.5	4219.0
2017	20,986.0	19,112.5	4343.0	331.6	40,098.5	4674.6
2018	21,057.0	20,326.0	4677.5	344.5	41,383.0	5022.0
2019	24,886.0	21,928.5	5026.3	764.5	46,814.5	5790.8
2020	23,353.0	19,655.5	5912.5	275.0	43,008.5	6187.5
2021	20,408.0	20,862.5	8370.8	218.0	41,270.5	8588.8
2022	20,408.0	20,862.5	8200.0	210.0	41,270.5	8410.0
2023	19,704.0	21,431.3	8050.0	200.0	41,135.3	8250.0
2024	19,000.0	22,000.0	7900.0	190.0	41,000.0	8090.0

by short-term rainfall trends. An exploratory Pearson correlation further reinforced this pattern, showing weak and non-significant associations between annual rainfall and total horticultural production in both sub-zobas. This aligns with Owusu et al. [54], who demonstrated that small reservoirs in West Africa stabilize agricultural production, and Aguilar et al. [2], who highlighted the role of irrigation and secure water access in building resilience to water scarcity. The findings also reflect long-term strategic investments in water infrastructure in Eritrea, including the construction of numerous small, medium, and large dams, which played a transformative role in expanding irrigation and promoting agricultural self-sufficiency [4]. This has been part of the government's broader self-reliance and food security agenda, aimed at adapting to the erratic rainfall patterns of the country [43, 46, 71]. Similar findings were reported in the Kilombero Valley of Tanzania, where local investments in smallholder irrigation infrastructure significantly influenced land use change, enabling more intensive and stable cultivation in irrigated areas compared to the wider landscape [3]. Hence, the increase in irrigated land in both sub zobas is best explained as an outcome of sustained policy interventions and infrastructural development aimed at enhancing resilience and ensuring long-term water and food security.

The trend of change in the horticultural price index and the irrigated area of both Dighe and Gala Nefhi shows a distinct divergence: while irrigated land expanded steadily, the price index declined Substantially after 2015 and remained below the baseline throughout the study period. This inverse relationship suggests that irrigation development in these sub zobas was not driven by short-term market incentives, but rather by structural and institutional factors such as public investment in water infrastructure and policy support focused on food security and agricultural resilience. This aligns with the findings of Pittock et al. [56], who proposed the need for systemic interventions, such as institutional reform, investment in maintenance, and capacity building, to sustain irrigation outcomes beyond economic returns. Similarly, Shah et al. [64] highlighted that in Sub-Saharan Africa, irrigation expansion is often driven by farmer-led initiatives supported by favorable government policies and donor programs, rather than fluctuations in crop prices. These broader regional insights reinforce the interpretation that non-market drivers, such as land availability, water access, and extension services, play a pivotal role in shaping irrigation patterns.

The findings highlight that the expansion of irrigated agriculture in Eritrea has been shaped more by long-term policy, infrastructure, and institutional factors than by short-term economic or climatic signals. This underscores the importance of integrated planning that combines physical investment with farmer support systems to ensure sustainable agricultural development in semi-arid environments.

5 Conclusion and Recommendations

This study demonstrates the practical use of remotely sensed data to quantify the change in irrigated fields in two distinct agroecological areas of Eritrea between 2015 and 2024 and links it with rainfall patterns, production data, and price fluctuations. The study revealed significant irrigation expansion in both areas, with notable differences in productivity outcomes. In Dighe, though there is a huge expansion in irrigated area, horticultural yields remained inconsistent, likely due to limited extension

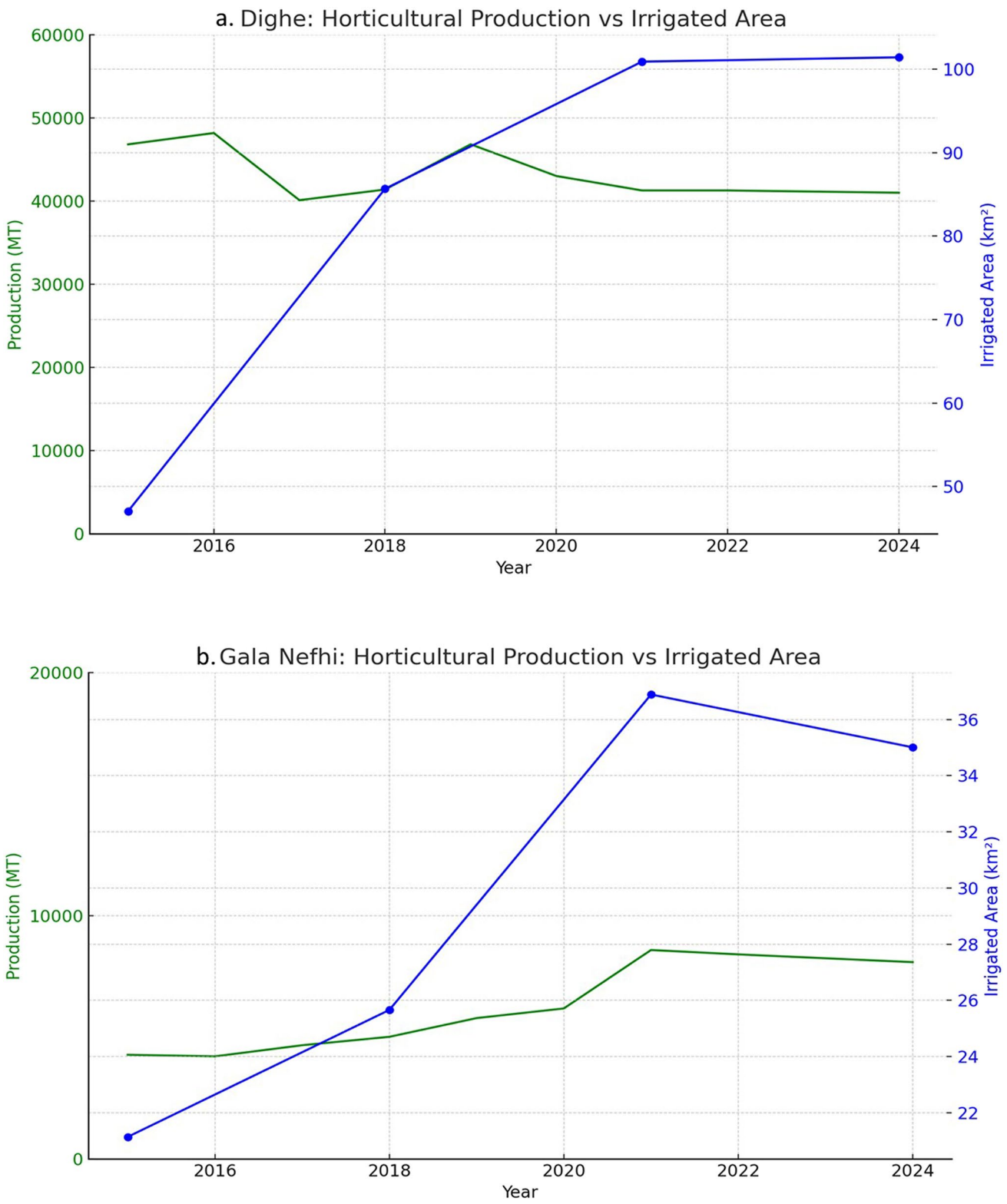

Fig. 9 Trends in horticultural production and irrigated area (a) Dighe and (b) Gala Nefhi from 2015 to 2024

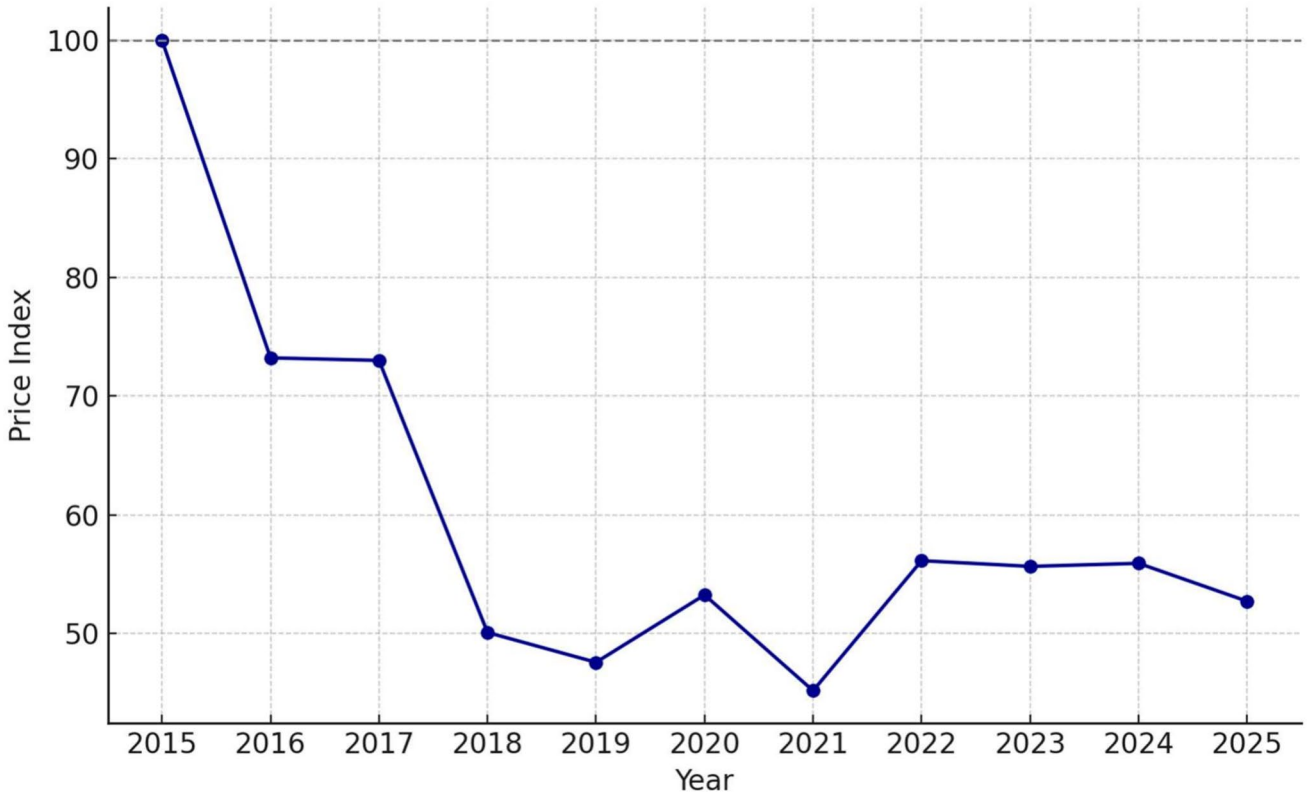

Fig. 10 Horticultural Crops Price Index from 2015 to 2025 (2015 (base year) = 100), based on mean annual prices of five dominant crops in the Asmara market. (Source: Ministry of Agriculture Reports 2025)

support and greater climatic variability. In contrast, Gala Nefhi exhibited a more synchronized trend between irrigation growth and output, supported by reliable micro-dam infrastructure and a relatively stable agro-climatic context.

The analysis was limited by the resolution of satellite imagery, lack of detailed socio-economic data, and the focus on only two sub zobas, which may not fully reflect national trends. To build on these findings, future research should employ higher-resolution and multi-temporal satellite imagery to capture crop phenology and seasonal variability more accurately and incorporate larger, well-distributed training datasets for improved classification and interpretation. Future studies are also encouraged to disaggregate horticultural production by crop type, to better understand crop-specific water demands and irrigation patterns. Additionally, more frequent and detailed data can help identify factors that influence irrigation expansion using inferential statistics.

From a policy and practice standpoint, irrigation interventions must include micro-dam optimization, groundwater recharge coupled with robust extension services, timely input supply, and better market access. Climate adaptation strategies, such as drought-tolerant crop varieties, localized water budgeting, and early warning systems, are also essential to buffer against rainfall variability, build national food system resilience, and ensure the sustainability of horticultural production.

Author Contribution BH: conceptualization, data curation, methodology, software, analysis, visualization, writing – original draft. AR: conceptualization, methodology, validation, review & editing- draft paper, supervision. AD: conceptualization, methodology, validation, review & editing- draft paper, supervision. MQ: conceptualization, data curation, methodology, software, analysis, review & editing- draft paper. All authors reviewed the manuscript.

Funding Open access funding provided by University of Pretoria. This research was funded by the Ministry of Agriculture, Eritrea, through the Integrated Agriculture Development Project (IADP), supported by the International Fund for Agricultural Development (IFAD), under Grant Number 2000002081. The University of Pretoria also provided open access funding.

Data Availability The data used in this research are available from the corresponding author upon reasonable request.

Declarations

Competing interests The authors declare no competing interests.

References

1. Afaq Y, Manocha A (2021) Analysis on change detection techniques for remote sensing applications: a review. Ecol Inform 63:101310. https://doi.org/10.1016/j.ecoinf.2021.101310
2. Aguilar FX, Hendrawan D, Cai Z, Roshetko JM, Stallmann J (2022) Smallholder farmer resilience to water scarcity. Environ Dev Sustain. https://doi.org/10.1007/s10668-021-01545-3
3. Alavaisha E, Mbande V, Börjeson L, Lindborg R (2021) Effects of land use change related to small-scale irrigation schemes in Kilombero Wetland Tanzania. Front Environ Sci 9(July):1–13. https://doi.org/10.3389/fenvs.2021.611686
4. Alemngus A, Amlesom S, Bovas JJL (2017) An overview of Eritrea's water resources. Int J Eng Res Dev 13(3):74–84
5. Arpitha M, Ahmed SA, Harishnaika N (2023) Land use and land cover classification using machine learning algorithms in Google Earth Engine. Earth Sci Inform 16(4):3057–3073. https://doi.org/10.1007/s12145-023-01073-w
6. Baret F, Guyot G (1991) Potentials and limits of vegetation indices for LAI and APAR assessment. Remote Sens Environ 35(2–3):161–173. https://doi.org/10.1016/0034-4257(91)90009-U
7. Bolognesi SF, Pasolli E, Belfiore OR, De Michele C, & D'Urso G (2020) Harmonized landsat 8 and sentinel-2 time series data to detect irrigated areas: an application in Southern Italy. *Remote Sensing*, *12*(8). https://doi.org/10.3390/RS12081275
8. Brown ME, Tondel F, Essam T, Thorne JA, Mann BF, Leonard K, Stabler B, Eilerts G (2012) Country and regional staple food price indices for improved identification of food insecurity. Glob Environ Change 22(3):784–794. https://doi.org/10.1016/j.gloenvcha.2012.03.005
9. Chabalala Y, Adam E, Ali KA (2022) Machine learning classification of fused Sentinel-1 and Sentinel-2 image data towards mapping fruit plantations in highly heterogenous landscapes. Remote Sensing 14(11):1–26. https://doi.org/10.3390/rs14112621
10. Congalton RG (1991) A review of assessing the accuracy of classifications of remotely sensed data. Remote Sens Environ 37(1):35–46. https://doi.org/10.1016/0034-4257(91)90048-B
11. Congalton RG, & Green K (2019) *Assessing the accuracy of remotely sensed data: principles and practices* (3rd ed.). CRC Press. https://doi.org/10.1201/9780429052729
12. Congalton RG, Oderwald RG, Mead RA (1983) Assessing Landsat classification accuracy using discrete multivariate analysis statistical techniques. Photogramm Eng Remote Sensing 49(12):1671–1678
13. Dash P, Sanders SL, Parajuli P, Ouyang Y (2023) Improving the accuracy of land use and land cover classification of landsat data in an agricultural watershed. Remote Sensing 15(16):1–24. https://doi.org/10.3390/rs15164020
14. Department of Land (DoL) (1997) Agro-ecological map of Eritrea [Map]. Asmara, Eritrea: Ministry of Land, Water and Environment. https://www.researchgate.net/figure/Map-showing-AEZ-in-Eritrea-Pearl-millet-is-grown-in-Moist-low-lands-arid-highland-and-and_fig1_372770836. Accessed 18 July 2025
15. Dube SV (2023) Institutional arrangements and agricultural support systems accessible to independent irrigators in South Africa. *South African Journal of Agricultural Extension*, *51*(I). https://doi.org/10.17159/2413-3221
16. Ewunetu A, Abebe G (2025) Integrating Google Earth Engine and random forest for land use and land cover change detection and analysis in the upper Tekeze Basin. Earth Sci Inform 18(2):227. https://doi.org/10.1007/s12145-025-01750-y
17. FAO (2005) AQUASTAT country profile – Eritrea. https://openknowledge.fao.org/server/api/core/bitstreams/38eef7f8-c372-4b4b-a8f4-953b05654f73/content#:~:text=Moisthighlandzone,38.7. Accessed 25 Apr 2025
18. FAO. (2020). *Food outlook - biannual report on global food markets: June 2020* (Issue July). https://doi.org/10.4060/ca9509e%0AThe
19. FAO (2021) Review of FAO's country programme in Eritrea 2017–2021. https://openknowledge.fao.org/server/api/core/bitstreams/d6f0a536-8200-4c1d-b853-f9b18e1a4be2/content. Accessed 21 Apr 2025
20. Farooq M, Mushtaq F, Yousuf U (2024) Estimation of loss in arable land and irrigation requirements using high-resolution imagery and Google Earth Engine. Irrig Drain 73(3):1151–1167. https://doi.org/10.1002/ird.2931
21. Foody GM (2020) Explaining the unsuitability of the kappa coefficient in the assessment and comparison of the accuracy of thematic maps obtained by image classification. Remote Sens Environ 239:111630. https://doi.org/10.1016/j.rse.2019.111630
22. Foster T, Mieno T, Brozović N (2020) Satellite-based monitoring of irrigation water use: assessing measurement errors and their implications for agricultural water management policy. Water Resour Res 56(11):1–19. https://doi.org/10.1029/2020WR028378
23. Ghebrezgabher MG, Yang T, Yang X, Wang C (2019) Assessment of desertification in Eritrea: land degradation based on Landsat images. J Arid Land 11(3):319–331. https://doi.org/10.1007/s40333-019-0096-4
24. Gu Z, & Zeng M (2024) The use of artificial intelligence and satellite remote sensing in land cover change detection: review and perspectives. *Sustainability (Switzerland)*, *16*(1). https://doi.org/10.3390/su16010274
25. Haile BT, Dougill AJ, Ramoelo A, Kidane TT (2025) Assessing farm-level sustainability : a comparative analysis of horticultural production systems in Eritrea. Front Sustain Food Syst 9:1532356. https://doi.org/10.3389/fsufs.2025.1532356
26. Huete A, Didan K, Miura T, Rodriguez E, Gao X, Ferreira L (2002) Overview of the radiometric and biophysical performance of the MODIS vegetation indices. Remote Sens Environ 83:195–213. https://doi.org/10.1016/S0034-4257(02)00096-2
27. Ihemezie EJ, Onunka CN, Umaru II (2020) The implication of agricultural land-use change on food security in Benue state, Nigeria. J Trop Agric 57(2):105–113. https://jtropag.kau.in/index.php/ojs2/article/view/777/515. Accessed 30 May 2023
28. Jensen JR (2015) Introductory digital image processing: a remote sensing perspective, 4th edn. Boston, MA: Pearson Education, Inc
29. Kaur N, Prakash R, & Diwakar M (2024) LULC Classification of Sentinel-2 satellite image using random forest algorithm in Google Earth engine. *Proceed - 4th Int Conf Technol Adv Comput Sci, ICTACS 2024*, 1390–1394. https://doi.org/10.1109/ICTACS62700.2024.10840515
30. Kebede E, Oluoch KO, Siebert S, Hartman S, Mehta P, Jägermeyr J, Ray D, Ali T, Brauman KA, Deng Q, Xie W, Davis KF (2025) A global open-source dataset of monthly irrigated and rainfed

cropped areas (MIRCA-OS) for the 21st century. Scientific Data 12(208):1–28. https://doi.org/10.1038/s41597-024-04313-w
31. Koech R, Haase M, Grima B, Taylor B (2021) Barriers and measures to improve adoption of irrigation technologies: a case study from the Bundaberg region in Queensland, Australia. Irrig Drain 70(4):909–923. https://doi.org/10.1002/ird.2583
32. Lambert MJ, Traoré PCS, Blaes X, Baret P, Defourny P (2018) Estimating smallholder crops production at village level from Sentinel-2 time series in Mali's cotton belt. Remote Sens Environ 216:647–657. https://doi.org/10.1016/j.rse.2018.06.036
33. Li Z, Chen X, Qi J, Xu C, An J, Chen J (2023) Accuracy assessment of land cover products in China from 2000 to 2020. Sci Rep 13(1):1–11. https://doi.org/10.1038/s41598-023-39963-0
34. Lu D, Weng Q (2007) A survey of image classification methods and techniques for improving classification performance. Int J Remote Sens 28(5):823–870. https://doi.org/10.1080/01431160600746456
35. Magidi J, Nhamo L, Mpandeli S, Mabhaudhi T (2021) Application of the random forest classifier to map irrigated areas using Google Earth Engine. Remote Sens 13(5):1–15. https://doi.org/10.3390/rs13050876
36. Masters WA, Bai Y, Herforth A, Sarpong DB, Mishili F, Kinabo J, Coates JC (2018) Measuring the affordability of nutritious diets in Africa: price indexes for diet diversity and the cost of nutrient adequacy. Am J Agric Econ 100(5):1285–1301. https://doi.org/10.1093/ajae/aay059
37. Maxwell AE, Warner TA, Fang F (2018) Implementation of machine-learning classification in remote sensing: an applied review. Int J Remote Sens 39(9):2784–2817. https://doi.org/10.1080/01431161.2018.1433343
38. McFEETERS SK (1996) The use of the normalized difference water index (NDWI) in the delineation of open water features. Int J Remote Sens 17(7):1425–1432. https://doi.org/10.1080/01431169608948714
39. McHugh ML (2012) Interrater reliability : the kappa statistic. Biochem Med 22(3):276–282
40. Measho S, Chen B, Pellikka P, Trisurat Y, Guo L, Sun S, Zhang H (2020) Land use/land cover changes and associated impacts on water yield availability and variations in the Mereb-Gash River Basin in the Horn of Africa. J Geophys Res Biogeosci 125(7):1–16. https://doi.org/10.1029/2020JG005632
41. Mehari Haile A (2007) A tradition in transition: water management reforms and indigenous spate irrigation systems in Eritrea. https://unesdoc.unesco.org/ark:/48223/pf0000153554. Accessed 16 June 2025
42. Ministry of Agriculture (MoA) (2022) The state of Eritrea: annual report 2021 [Unpublished report]. Ministry of Agriculture, Asmara, Eritrea
43. MoA (2023) National report submitted to the United Nations Convention to Combat Desertification (UNCCD) – Seventh reporting cycle (Issue March). https://www.unccd.int/our-work-impact/country-profiles/eritrea/country-report/2022. Accessed 07 June 2025
44. Mohammed M, Birhanu B, Abegaz F (2023) Multi-spectral remote sensing for current irrigated area mapping of the Rift Valley Lakes Basin in Ethiopia. Aqua Water Infrastruct, Ecosyst Soc 72(12):2396–2407. https://doi.org/10.2166/aqua.2023.413
45. MohanRajan SN, Loganathan A, Manoharan P (2020) Survey on land use/land cover (LU/LC) change analysis in remote sensing and GIS environment: techniques and challenges. Environ Sci Pollut Res Int 27(24):29900–29926. https://doi.org/10.1007/s11356-020-09091-7
46. MoLWE (2007) State of Eritrea national adaptation programme of action (Issue April). https://unfccc.int/resource/docs/napa/eri01.pdf. Accessed 07 June 2025
47. MoLWE (2008) Action plan for integrated water resource management (IWRM) in Eritrea (Issue December). https://www.gwp.org/globalassets/global/toolbox/about/iwrm/africa/eritrea-iwrm-action-plan.pdf. Accessed 07 June 2025
48. Muluneh A, Tadesse T, Girma R (2022) Assessing potential land suitable for surface irrigation using GIS and AHP techniques in the Rift Valley Lakes Basin. Ethiopia Sustain Water Resour Manag 8(2):1–22. https://doi.org/10.1007/s40899-022-00632-1
49. Munthali MG, Davis N, Adeola AM, Botai JO, Kamwi JM, Chisale HLW, Orimoogunje OOI (2019) Local perception of drivers of land-use and land- cover change dynamics across Dedza district, Central Malawi region. Sustainability. https://doi.org/10.3390/su11030832
50 Musa MK, Odera PA (2015) Land Use Land Cover Changes and their effects on agricultural land: a case study of Kiambu County - Kenya. Kabarak J Res Innov 3(1):74–86. https://doi.org/10.58216/kjri.v3i1.15
51. Negede O, Karanja FN (2025) Modelling land degradation (LD) using geospatial techniques for agricultural and environmental management case study: Alla Catchment; Dekemhare-Eritrea. J Geogr Inf Syst 17(1):97–117. https://doi.org/10.4236/jgis.2025.171006
52. Ogbazghi W, Stillhardt B, Herweg K (2011) Sustainable land management – a textbook with a focus on Eritrea. In: Wachs T, Kohler T (eds) Geographica Bernensia and Hamelmalo Agricultural College. https://www.researchgate.net/publication/279884733_Sustianbale_Land_Management_a_Textbook_with_focus_on_Eritrea. Accessed 25 Apr 2025
53. Ouattara B, Forkuor G, Zoungrana BJB, Dimobe K, Danumah J, Saley B, Tondoh JE (2020) Crops monitoring and yield estimation using sentinel products in semi-arid smallholder irrigation schemes. Int J Remote Sens 41(17):6527–6549. https://doi.org/10.1080/01431161.2020.1739355
54. Owusu S, Cofie O, Mul M, Barron J (2022) The significance of small reservoirs in sustaining agricultural landscapes in dry areas of West Africa: a review. Water (Switzerland) 14(9):1–21. https://doi.org/10.3390/w14091440
55. Ozdogan M, Yang Y, Allez G, Cervantes C (2010) Remote sensing of irrigated agriculture: opportunities and challenges. Remote Sens 2(9):2274–2304. https://doi.org/10.3390/rs2092274
56. Pittock J, Bjornlund H, van Rooyen A (2020) Transforming failing smallholder irrigation schemes in Africa: a theory of change. Int J Water Resour Dev 36(sup1):S1–S19. https://doi.org/10.1080/07900627.2020.1819776
57. Pontius RG, Millones M (2011) Death to Kappa: birth of quantity disagreement and allocation disagreement for accuracy assessment. Int J Remote Sens 32(15):4407–4429. https://doi.org/10.1080/01431161.2011.552923
58. R CoreTeam (2022) R: a language and environment for statistical computing (4.1.3). R Foundation for Statistical Computing. https://www.r-project.org/. Accessed 07 Oct 2024
59. Richardson G, Knudby A, Crowley MA, Sawada M, Chen W (2025) Machine learning approaches to landsat change detection analysis. Can J Remote Sens. https://doi.org/10.1080/07038992.2024.2448169
60. Rondeaux G, Steven M, Baret F (1996) Optimization of soil-adjusted vegetation indices. Remote Sens Environ 55(2):95–107. https://doi.org/10.1016/0034-4257(95)00186-7
61. Rouse JW, Haas RH, Schell JA, Deering DW (1974) Monitoring vegetation systems in the Great Plains with ERTS. In: NASA Special Publication, vol 351. https://ntrs.nasa.gov/api/citations/19740022614/downloads/19740022614.pdf. Accessed 30 May 2025
62. Said M, Hyandye C, Komakech HC, Mjemah IC, Munishi LK (2021) Predicting land use/cover changes and its association to agricultural

production on the slopes of Mount Kilimanjaro, Tanzania. Ann GIS 27(2):189–209. https://doi.org/10.1080/19475683.2020.1871406
63. Sarfo I, Qiao J, Yeboah E, Puplampu DA, Kwang C, Fynn IEM, Batame M, Appea EA, Hagan DFT, Ayelazuno RA, Boamah V, Sarfo BA (2024) Meta-analysis of land use systems development in Africa: trajectories, implications, adaptive capacity, and future dynamics. Land Use Policy 144(January):107261. https://doi.org/10.1016/j.landusepol.2024.107261
64. Shah T, Namara R, Rajan A (2020) Accelerating irrigation expansion in Sub-Saharan Africa policy lessons from the global revolution in farmer-led smallholder irrigation. https://hdl.handle.net/10986/35804. Accessed 16 June 2025
65. Siebert S, Hoogeveen J, Frenken K (2006) Irrigation in Africa, Europe and Latin America - update of the digital global map of irrigation areas to version 4. In: *Frankfurt Hydrology Paper* (Issue 05). https://www.researchgate.net/publication/235704701_Irrigation_in_Africa_Europe_and_Latin_America_Update_of_the_digital_global_map_of_irrigation_areas_to_Version_4. Accessed 16 June 2025
66. Stevens JB, Ntai PJ (2011) The role of extension support to irrigation farmers in Lesotho. S Afr J Agric Ext 39(2):104–112
67. Su Q, Lv J, Fan J, Zeng W, Pan R, Liao Y, Song Y, Zhao C, Qin Z, Defourny P (2023) Remote sensing-based classification of winter irrigation fields using the random forest algorithm and GF-1 data: a case study of Jinzhong Basin. North China Remote Sensing 15(18):1–16. https://doi.org/10.3390/rs15184599
68. Thenkabail PS, Biradar CM, Noojipady P, Dheeravath V, Li Y, Velpuri M, Gumma M, Gangalakunta ORP, Turral H, Cai X, Vithanage J, Schull MA, Dutta R (2009) Global irrigated area map (GIAM), derived from remote sensing, for the end of the last millennium. Int J Remote Sens 30(14):3679–3733. https://doi.org/10.1080/01431160802698919
69. Wang L, Yan J, Ma J, Huang X, Li J, Wang S, He H, Long A, & Zhang X (2024) Cloud computing in remote sensing: a comprehensive assessment of state of the arts. In P. S. Thenkabail (Ed.), *Remote Sensing Handbook Volume 1* (2nd ed., pp. 399–438). CRC Press. https://doi.org/10.1201/9781003541141
70. Weitkamp T, Jan Veldwisch G, Karimi P, de Fraiture C (2023) Mapping irrigated agriculture in fragmented landscapes of sub-Saharan Africa: an examination of algorithm and composite length effectiveness. Int J Appl Earth Obs Geoinf 122(April):103418. https://doi.org/10.1016/j.jag.2023.103418
71. Weldetsion GG (2023) *Eritrea's self-reliance policy and the road to sustainable food and water security* [SOAS University of London]. https://doi.org/10.25501/SOAS.00040447
72. Xiang K, Yuan W, Wang L, Deng Y (2020) An LSWI-based method for mapping irrigated areas in China using moderate-resolution satellite data. Remote Sens 12(24):1–15. https://doi.org/10.3390/rs12244181
73. Xu H (2006) Modification of normalised difference water index (NDWI) to enhance open water features in remotely sensed imagery. Int J Remote Sens 27(14):3025–3033. https://doi.org/10.1080/01431160600589179
74. Yimer AK, Haile AT, Hatiye SD, Ragettli S, Taye MT (2024) Comparative evaluation of the accuracy of mapping irrigated areas using sentinel 1 images in the Bilate and Gumara watersheds, Ethiopia. Cogent Engineering. https://doi.org/10.1080/23311916.2024.2357728
75. Yonaba R, Koïta M, Mounirou LA, Tazen F, Queloz P, Biaou AC, Niang D, Zouré C, Karambiri H, Yacouba H (2021) Spatial and transient modelling of land use/land cover (LULC) dynamics in a Sahelian landscape under semi-arid climate in northern Burkina Faso. Land Use Policy. https://doi.org/10.1016/j.landusepol.2021.105305
76. Zha Y, Gao J, Ni S (2003) Use of normalized difference built-up index in automatically mapping urban areas from TM imagery. Int J Remote Sens 24(3):583–594. https://doi.org/10.1080/01431160304987